Macroscopic superpositions of Bose-Einstein condensates

Janne Ruostekoski,[1] M. J. Collett,[1] Robert Graham,[2] and Dan F. Walls[1]

[1]*Department of Physics, University of Auckland, Private Bag 92019, Auckland, New Zealand*
[2]*Universität-GH-Essen, Fachbereich Physik, D45117 Essen, Germany*

(Received 15 July 1997)

We consider two dilute gas Bose-Einstein condensates with opposite velocities from which a monochromatic light field detuned far from the resonance of the optical transition is coherently scattered. In the thermodynamic limit, when the relative fluctuations of the atom number difference between the two condensates vanish, the relative phase between the Bose-Einstein condensates may be established in a superposition state by detections of spontaneously scattered photons, even though the condensates have initially well-defined atom numbers. For a finite system, stochastic simulations show that the measurements of the scattered photons lead to a randomly drifting relative phase and drive the condensates into entangled superpositions of number states. This is because according to Bose-Einstein statistics the scattering to an already occupied state is enhanced. [S1050-2947(97)08012-8]

PACS number(s): 03.75.Fi, 03.65.Bz, 42.50.Vk, 05.30.Jp

I. INTRODUCTION

Bose-Einstein condensates (BEC's) of ultracold trapped atomic gases [1–4] have stimulated interest in the coherence properties of matter. BEC's are expected to exhibit a macroscopic quantum coherence which in thermal atomic ensembles is absent. Even BEC's with a well-defined number of atoms, and with no phase information, could show phase correlations in particular measurement processes on atoms [5–11] or on photons [12]. The relative phase between two BEC's could be determined, for instance, by various optical methods [12–16]. In recent experiments Andrews *et al.* [17] have found evidence of macroscopic quantum coherence in a BEC by measurements of the interference of two condensates by absorption imaging. The two independent and spatially separated BEC's were created by a repulsive optical force in the center of the trap.

In this paper we consider an optical analogue of the atom detection schemes of two BEC's in different momentum states [5–7,9]. Instead of looking at the spatial interference pattern we combine the scattered photons from the atomic transitions between different BEC's with a photon beam splitter. The measurements on scattered light have evident advantages over atom counting from a theoretical point of view. In the case of light scattering we can use the well-known theories of photon detection [18]. Also, the measurement of spontaneously scattered photons is nondestructive for the condensates, because only light is scattered and no atoms are removed from the two BEC's. In our measurement scheme it is shown via the simulations of stochastic Schrödinger equations that the detections of spontaneously scattered photons drive the condensates into macroscopic quantum superpositions of phase and number states ("Schrödinger cats"). The phase superpositions are a consequence of the particular measurement process, which is insensitive to certain phase values. The entangled number state superpositions follow from the properties of Bose-Einstein statistics and from the macroscopic quantum coherence of BEC's. The number state superpositions are multiparticle quantum states with spatially nonlocal correlations. Due to

the large fluctuations of the number difference between the BEC's the relative phase drifts randomly in the case of a finite system and no stable phase is built up by measurements. The fluctuations of the number difference vanish in the thermodynamic limit and the measurements establish a stable phase.

Recently, Cirac *et al.* [19] have studied the ground state of two coupled BEC's by variational techniques. They have found that under certain conditions the state with a minimum energy corresponds to a macroscopic superposition of number states.

We begin in Sec. II A by introducing basic relations. In the limit of large detuning of the driving light field from the atomic resonance the excited state operators may be eliminated adiabatically. We obtain an effective two-state Hamiltonian coupling the two BEC's. We study the dynamics of the system in terms of stochastic trajectories of state vectors. In Sec. II B we consider the thermodynamic limit, where the fluctuations of the number difference between the BEC's vanish. The results of simulations for a finite system are presented in Sec. II C. In Sec. II D we show that the number state superpositions could be detected by considering the intensity correlations of the scattered light. Finally, a few concluding remarks are made in Sec. III.

II. OPEN SYSTEM DYNAMICS

A. Basic relations

The internal quantum state for both condensates is denoted by $|g\rangle$. This state is optically coupled to the electronically excited state $|e\rangle$ by the driving electric field $\mathbf{E}_d$ with a dominant frequency Ω. The light field is assumed to be in a coherent state and detuned far from the resonance of the atomic transition. The two BEC's are assumed to be optically thin [20] and in the momentum states $\mathbf{k}_0$ and $-\mathbf{k}_0$. We consider the situation in which the condensates are overlapping when the light is switched on. We only consider the coherent spontaneous scattering between the condensates, which is stimulated by a large number of atoms in the condensates. By spontaneous scattering we mean that the emis-

sion is not stimulated by light, although it is stimulated by atoms. The decay into noncondensate center-of-mass (c.m.) states is also stimulated by the Bose-Einstein statistics. However, at very low temperatures this stimulation is much weaker because most of the particles are in the condensates. In addition to the Bose stimulation of spontaneous emission there is unstimulated free-space decay, at rate γ, which is always present. With a sufficiently large number of atoms in the two BEC's the free-space decay may be ignored.

The annihilation operators for the two BEC's are $g_{\mathbf{k}_0}$ and $g_{-\mathbf{k}_0}$. Here $g_{\mathbf{k}_0}$ denotes the annihilation operator for the electronic ground state $|g\rangle$ and the c.m. state $\mathbf{k}_0$ with the corresponding wave function $\phi_{g,\mathbf{k}_0}(\mathbf{r})$. To simplify the notation we define $b \equiv g_{\mathbf{k}_0}$, $\phi_b(\mathbf{r}) \equiv \phi_{g,\mathbf{k}_0}(\mathbf{r})$, $c \equiv g_{-\mathbf{k}_0}$, and $\phi_c(\mathbf{r}) \equiv \phi_{g,-\mathbf{k}_0}(\mathbf{r})$. We obtain for the Hamiltonian [20,21]

$$
\begin{aligned}
H = &\; \hbar \epsilon^g_{\mathbf{k}_0} b^\dagger b + \hbar \epsilon^g_{-\mathbf{k}_0} c^\dagger c + \sum_{\mathbf{k}} \hbar(\omega_{eg} + \epsilon^e_{\mathbf{k}}) e^\dagger_{\mathbf{k}} e_{\mathbf{k}} \\
&+ \sum_q \hbar \omega_q a^\dagger_q a_q \\
&- \sum_{\mathbf{k}} \left(\int d^3r\, \mathbf{d}_{ge} \cdot \mathbf{E}(\mathbf{r}) \phi^*_b(\mathbf{r}) \phi_{e\mathbf{k}}(\mathbf{r}) b^\dagger e_{\mathbf{k}} + \mathrm{H.c.} \right) \\
&- \sum_{\mathbf{k}} \left(\int d^3r\, \mathbf{d}_{ge} \cdot \mathbf{E}(\mathbf{r}) \phi^*_c(\mathbf{r}) \phi_{e\mathbf{k}}(\mathbf{r}) c^\dagger e_{\mathbf{k}} + \mathrm{H.c.} \right),
\end{aligned}
\tag{1}
$$

where the excited state wave function for the c.m. state $\mathbf{k}$ is $\phi_{e\mathbf{k}}$. The dispersion relations for the ground state and excited state c.m. frequencies are $\epsilon^g_{\mathbf{k}}$ and $\epsilon^e_{\mathbf{k}}$, respectively. The photon annihilation operator for the mode q is a_q. The internal atomic energy is described by the frequency ω_{eg} of the optical transition between the electronic ground state and excited state. The last two terms in Eq. (1) are for the atom-light dipole interaction. The dipole matrix element for the atomic transition $e \to g$ is given by $\mathbf{d}_{ge}$. We consider the translationally invariant system, where the eigenfunctions for the condensates are plane waves: $\phi_b(\mathbf{r}) = e^{i\mathbf{k}_0 \cdot \mathbf{r}}/\sqrt{V}$ and $\phi_c(\mathbf{r}) = e^{-i\mathbf{k}_0 \cdot \mathbf{r}}/\sqrt{V}$. The driving electric field is also described by a plane wave $\mathbf{E}^+_d(\mathbf{r}) = \mathcal{E}\, \hat{\mathbf{e}}\, e^{i(\mathbf{k} \cdot \mathbf{r} - \Omega t)}/2$.

In the limit of large detuning, $\Delta = \Omega - \omega_{eg}$, the excited state operators $e_{\mathbf{k}}$ in Eq. (1) may be eliminated adiabatically, and the c.m. energies of the excited state may be ignored [20]. The system may then be described by an effective two-state Hamiltonian:

$$
\begin{aligned}
H = &\; \hbar \epsilon^g_{\mathbf{k}_0} b^\dagger b + \hbar \epsilon^g_{-\mathbf{k}_0} c^\dagger c + \sum_q \hbar \omega_q a^\dagger_q a_q \\
&- \frac{1}{\hbar \Delta} \bigg\{ \hat{N} \int d^3r\, \mathbf{d}_{ge} \cdot \mathbf{E}(\mathbf{r}) \mathbf{d}_{eg} \cdot \mathbf{E}(\mathbf{r}) \phi^*_b(\mathbf{r}) \phi_b(\mathbf{r}) \\
&+ \left(b^\dagger c \int d^3r\, \mathbf{d}_{ge} \cdot \mathbf{E}(\mathbf{r}) \mathbf{d}_{eg} \cdot \mathbf{E}(\mathbf{r}) \phi^*_b(\mathbf{r}) \phi_c(\mathbf{r}) + \mathrm{H.c.} \right) \bigg\}.
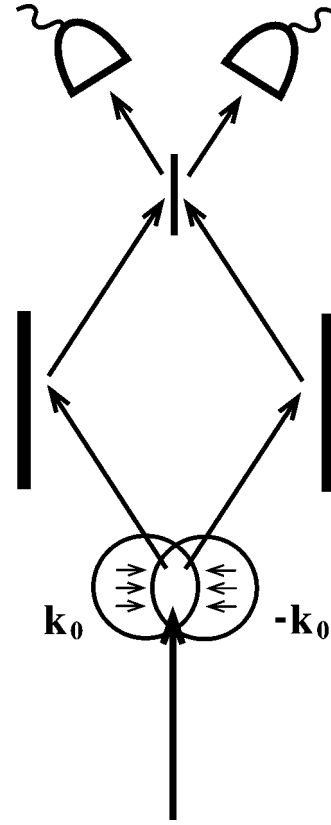\end{aligned}
\tag{2}
$$

FIG. 1. The experimental setup. The incoming light field is scattered from two overlapping BEC's moving with opposite velocities. The atoms scattering from one condensate to another change the momenta of the scattered photons. The scattered photons are collected by reflective mirrors and a 50-50 beam splitter. The photons are detected from the two output channels of the beam splitter. The photons scattered forward introduce only a constant phase shift and they are ignored.

Here we have used the fact that for the plane waves $\phi^*_b(\mathbf{r}) \phi_b(\mathbf{r}) = \phi^*_c(\mathbf{r}) \phi_c(\mathbf{r})$. The total atom number operator is given by $\hat{N} = b^\dagger b + c^\dagger c$. Because the total number is conserved, the operator $\hat{N}$ contributes to the measurements only through a constant phase shift. Thus, we may ignore the term proportional to $\hat{N}$ in Eq. (2).

We consider the dynamics of the two BEC's and the driving light field as an open quantum system and eliminate the vacuum electromagnetic fields. The setup of our gedanken experiment is given in Fig. 1. The incoming light field is scattered from two overlapping BEC's moving with opposite velocities. The scattering processes in which an atom scatters back to the same condensate introduce the term proportional to the total number of atoms in Eq. (2), and they may be ignored. In the scattering processes in which atoms scatter between different condensates the light beams are deflected due to the recoil momentum. In Fig. 1 a photon deflected to the left corresponds to the change of the momentum of an atom from $-\mathbf{k}_0$ to $\mathbf{k}_0$, i.e., the amplitude of the scattered electric field is proportional to $b^\dagger c$. Similarly, a photon deflected to the right corresponds to the change of the momentum of an atom upon scattering from $\mathbf{k}_0$ to $-\mathbf{k}_0$. In this case the amplitude of the scattered electric field is proportional to $c^\dagger b$. The scattered light beams are combined by perfectly

reflecting mirrors and a 50-50 photon beam splitter. The detection rate of photons on the detectors is the intensity of the scattered light $I(r) = 2c\epsilon_0 \langle \mathbf{E}^-(\mathbf{r}) \cdot \mathbf{E}^+(\mathbf{r}) \rangle$ integrated over the scattering directions divided by the energy of a photon $\hbar c k$. Writing the electric fields in the far radiation zone $(kr \gg 1)$ [20] we obtain the detection rate at the channel j:

$$\gamma_j = \frac{1}{\hbar c k} \int d\Omega_{\hat{\mathbf{n}}} \, r^2 I_j(\mathbf{r}) = 2\Gamma \langle C_j^\dagger C_j \rangle, \qquad (3)$$

$$\Gamma \equiv \frac{3\gamma}{16\pi\hbar^2\Delta^2} |d_{eg}\mathcal{E}|^2, \qquad (4)$$

where the linewidth of the electric dipole transition is given by $\gamma = d_{eg}^2 k^3 / (6\pi\hbar\epsilon_0)$. The two relaxation channels corresponding to the two output channels of the beam splitter are

$$C_1 = \hat{J}_x, \quad C_2 = \hat{J}_y, \qquad (5)$$

where the familiar angular momentum operators obeying SU(2) algebra are defined by

$$\hat{J}_x = \frac{1}{2}(b^\dagger c + c^\dagger b), \qquad (6a)$$

$$\hat{J}_y = \frac{1}{2i}(b^\dagger c - c^\dagger b), \qquad (6b)$$

$$\hat{J}_z = \frac{1}{2}(b^\dagger b - c^\dagger c), \qquad (6c)$$

and $\hat{J}^2 = \hat{J}_x^2 + \hat{J}_y^2 + \hat{J}_z^2 = (\hat{N}/2 + 1)\hat{N}/2$ is the Casimir invariant.

The system Hamiltonian for the BEC's and for the driving electromagnetic field is eliminated completely in the interaction representation and according to Ref. [12] we may then write down the equation of motion for the reduced density matrix of the system in the limit of large detuning of the driving light from the atomic resonance

$$\dot{\rho}_S = -\Gamma \sum_{i=1}^2 (C_i^\dagger C_i \rho_S + \rho_S C_i^\dagger C_i - 2 C_i \rho_S C_i^\dagger). \qquad (7)$$

If we assume the condensates to be in coherent states with equal mean atom numbers $\langle b \rangle = \sqrt{N/2} e^{i\varphi_b}$ and $\langle c \rangle = \sqrt{N/2} e^{i\varphi_c}$, the intensities of the scattered light in the two channels are

$$I_1 \propto \langle \hat{J}_x^2 \rangle \propto (\cos\varphi)^2, \quad I_2 \propto \langle \hat{J}_y^2 \rangle \propto (\sin\varphi)^2. \qquad (8)$$

Here we have defined the value of the relative phase by $\varphi \equiv \varphi_c - \varphi_b$, where φ_b and φ_c are the macroscopic phases of the condensates b and c, respectively. There is an ambiguity in Eq. (8) between the phase values $\pm\varphi$ and $\pi \pm \varphi$. For phase-sensitive homodyne detection this ambiguity vanishes.

The dynamics of the density operator from Eq. (7) may be unraveled into stochastic trajectories of state vectors [22–24]. The procedure consists of the evolution of the system with a non-Hermitian Hamiltonian H_{eff}, and randomly decided quantum "jumps" corresponding to the direct detections of spontaneously emitted photons. The system evolu-

tion is thus conditioned on the outcome of a measurement. The non-Hermitian Hamiltonian is obtained from Eq. (7),

$$H_{\text{eff}} = -i\hbar\Gamma \sum_{j=1}^2 C_j^\dagger C_j = -i\hbar\Gamma(\hat{J}^2 - \hat{J}_z^2). \qquad (9)$$

The non-Hermitian Hamiltonian H_{eff} determines the evolution of the state vector $\psi_{\text{sys}}(t)$. If the wave function $\psi_{\text{sys}}(t)$ is normalized, the probability that a photon from the output channel j ($j = 1,2$) of the beam splitter is detected during the time interval $[t, t + \delta t]$ is

$$P_j(t) = 2\Gamma \langle \psi_{\text{sys}}(t) | C_j^\dagger C_j | \psi_{\text{sys}}(t) \rangle \delta t. \qquad (10)$$

The probability of no detections is $1 - P_1 - P_2$.

The implementation of the simulation algorithm is similar to Ref. [12]. At the time t_0 we generate a quasirandom number ϵ which is uniformly distributed between 0 and 1. We assume that the state vector $\psi_{\text{sys}}(t_0)$ at the time t_0 is normalized. Then we evolve the state vector by the non-Hermitian Hamiltonian H_{eff} iteratively for finite time steps $\Delta t \simeq \delta t$. At each time step n we compare ϵ to the reduced norm of the wave function, until $\langle \psi_{\text{sys}}(t_0 + n\Delta t) | \psi_{\text{sys}}(t_0 + n\Delta t) \rangle < \epsilon$, when the detection of a photon occurs. After the detection we generate a new quasirandom number η. We evaluate P_1 and P_2 from Eq. (10) at the time of the detection. If $\eta < P_1/(P_1 + P_2)$ we say the photon has been detected from channel 1. If the photon has been observed during the time step $t \to t + \Delta t$ we take the new wave function at $t + \Delta t$ to be

$$|\psi_{\text{sys}}(t + \Delta t)\rangle = \sqrt{2\Gamma} \hat{J}_x |\psi_{\text{sys}}(t)\rangle, \qquad (11)$$

which is then normalized. Otherwise, $\eta > P_1/(P_1 + P_2)$ and the photon has been detected from channel 2. In that case the new wave function before the normalization reads

$$|\psi_{\text{sys}}(t + \Delta t)\rangle = \sqrt{2\Gamma} \hat{J}_y |\psi_{\text{sys}}(t)\rangle. \qquad (12)$$

After each detection the process starts again from the beginning.

B. Thermodynamic limit

Before presenting numerical results of the simulations of the stochastic Schrödinger equations, we investigate qualitatively the buildup of the macroscopic coherence by the measurement process in the limit $N \to \infty$. The eigenstates of the effective Hamiltonian H_{eff} in Eq. (9) are number states which have flat phase amplitudes. Thus, the time evolution of H_{eff} does not support any particular phase value over other values, and the relative phase between the two BEC's is determined by the distribution of the photon detections between the two output channels of the beam splitter. Because the two relaxation channels do not commute, $[\hat{J}_x, \hat{J}_y] = i\hat{J}_z$, the state of the system depends also on the particular order in which the scattered photons are detected. This complicates the analysis substantially. An evident simplification is to consider the thermodynamic limit $N \to \infty$, where the relative fluctuations of the number difference between the BEC's vanish $\langle \hat{J}_z \rangle / \langle \hat{N} \rangle \to 0$. In the next section we consider the numerical simulations of systems which are far away from this

limit. However, it turns out that the qualitative behavior of the macroscopic phases is still very similar.

In the thermodynamic limit we can replace the angular momentum operators $\hat{J}_x$ and $\hat{J}_y$ by $(\hat{N}/2)\cos\hat{\varphi}$ and $(\hat{N}/2)\sin\hat{\varphi}$, respectively, where $\hat{\varphi}$ is the relative phase operator between the two BEC's. Then the two relaxation channels in Eq. (5) commute, $[\cos\hat{\varphi},\sin\hat{\varphi}]=4i\Delta\hat{N}/\hat{N}^2\to 0$, and the relevant commutation relations are given by

$$[\Delta\hat{N},\cos\hat{\varphi}]=i\sin\hat{\varphi}, \quad [\Delta\hat{N},\sin\hat{\varphi}]=-i\cos\hat{\varphi}, \quad (13)$$

where we have written $\Delta\hat{N}\equiv\hat{J}_z$. Geometrically, the thermodynamic limit may be understood as a restriction of the dynamics of the angular momentum variables to the equator $\langle\hat{J}_z\rangle\simeq 0$ of the Bloch sphere, as the radius of the sphere goes to infinity.

Now we can use the procedure developed in Ref. [10]. To simplify the notation, we ignore the spatial dependence of the wave functions. We expand the number state $|N/2,N/2\rangle$ in terms of the overcomplete set of phase states [25]:

$$|\varphi\rangle_N=\frac{1}{\sqrt{2^N N!}}(b^\dagger e^{-i\varphi/2}+c^\dagger e^{i\varphi/2})^N|0\rangle. \quad (14)$$

An analysis similar to Ref. [10] then leads to the state of the system after n_1 and n_2 detections from output channels 1 and 2 of the beam splitter, respectively:

$$|\psi(n_1,n_2)\rangle\propto\int_0^{2\pi}d\varphi(\cos\varphi)^{n_1}(\sin\varphi)^{n_2}|\varphi\rangle_N. \quad (15)$$

The value of the phase φ that maximizes the integrand satisfies the relation $\tan^2\varphi=n_2/n_1$. If $0\leq\varphi_0\leq\pi/2$ is a solution for the maximum amplitude, then $-\varphi_0$ and $\pi\pm\varphi_0$ are also solutions. For $n_1,n_2\gg 1$, we can express the integrand in Eq. (15) in terms of exponential functions and expand the exponents in a Taylor series around $\pm\varphi_0$ and $\pi\pm\varphi_0$. We obtain

$$|\psi(n_1,n_2)\rangle\propto\int_0^{2\pi}d\varphi\{e^{-n(\varphi-\varphi_0)^2}+(-1)^{n_1}e^{-n(\pi-\varphi-\varphi_0)^2}$$

$$+(-1)^{n_1+n_2}e^{-n(\varphi+\pi-\varphi_0)^2}$$

$$+(-1)^{n_2}e^{-n(\varphi+\varphi_0)^2}\}|\varphi\rangle_N, \quad (16)$$

where $n=n_1+n_2$. The phase distributions are Gaussians centered at four superposition values $\pm\varphi_0$ and $\pi\pm\varphi_0$, where $0\leq\varphi_0\leq\pi/2$ is a solution for $\tan^2\varphi=n_2/n_1$. The phase is well defined with a narrow width for the Gaussian. The transition from the binomial distribution of Eq. (15) to the normal distribution of Eq. (16) is just the realization of the central limit theorem for a large number of detections, while the superpositions are a consequence of the particular detection method, which is insensitive to the phase values $\pm\varphi$ and $\pi\pm\varphi$ according to Eq. (8).

C. Numerical results

For a finite system the two relaxation channels from Eq. (5) do not commute and the state of the BEC's depends on the particular order in which photons from the two output channels of the beam splitter are detected. We have simulated the measurements of the spontaneously scattered photons numerically for $N=200$ atoms. Even though we start from the initial number state $N_b=N_c=100$ with no phase information, the detections establish coherence properties for BEC's similarly to Eq. (16). However, the value of the phase φ_0 in Eq. (16) does not stabilize due to the moderate value of N chosen, even for a large number of detections. The two BEC's are also in entangled number state superpositions. The coherence properties of the BEC's vary strongly even during single realizations of the measurement process. In the extreme case the condensates approach an entangled number state with almost all the atoms in one of the two BEC's.

The emergence of the number state superpositions may be understood from the quantum statistical properties of Bose-Einstein particles. Because the scattering to the noncondensate modes is ignored, the total number of atoms in the two BEC's is conserved and the atom numbers are entangled. According to Bose-Einstein statistics the scattering to an already occupied state is enhanced. For the initial state $|N/2,N/2\rangle$ the probability for light to scatter atoms between the two BEC's is, in the case of spatially overlapping condensates and in the limit of large numbers of atoms, approximately proportional to $(N/2)^2$. Because the detected photons corresponding to the two atomic transitions between the BEC's are indistinguishable, the number state distribution remains symmetric with respect to the initial state during the scattering process. For an entangled number state ($|N-k,k\rangle+|k,N-k\rangle)/\sqrt{2}$ the scattering probability is approximately proportional to $(N-k)k\leq(N/2)^2$. Hence the states with unequal atom numbers have smaller scattering rates and they are more stable. It should be pointed out that it is not necessary to have initially equal atom numbers to obtain number state superpositions, although the distributions are perfectly symmetric only if the initial atom numbers are the same.

The state of the BEC's may be described in terms of quasiprobability functions. For the number state distribution of atoms $|\psi_b\rangle=\Sigma_n c_n|n\rangle$ in the condensate b we have evaluated the Q function [26]:

$$Q(\alpha)=\frac{|\langle\alpha|\psi_b\rangle|^2}{\pi}=\frac{e^{-|\alpha|^2}}{\pi}\left|\sum_{n=0}^{N}\frac{\alpha^n c_n^*}{\sqrt{n!}}\right|^2. \quad (17)$$

In Figs. 2, 3, and 4, we have plotted $|\psi_b|$, the absolute value of the wave function in the condensate b in the number state basis, and the corresponding Q function at different times during a single realization of measurements. Figures 2 and 3 represent typically observed distributions, when several thousands of detections are made. In Fig. 4 we have a special case in which almost all the atoms are in one of the two BEC's. In Fig. 2(a) two distinct peaks in the number distribution are clearly observed. The first peak is centered at $N_b\simeq 30$ atoms, i.e., $N_c\simeq 170$ atoms, and the second at $N_b\simeq 170$ atoms, i.e., $N_c\simeq 30$ atoms. Only odd number states are occupied. This is because in each photon detection the states with only even numbers in the atom number distribution are changed to the states with only odd atom numbers and vice versa. In particular, for a coherent system we may define even $|\alpha,+\rangle$ and odd $|\alpha,-\rangle$ coherent states by $|\alpha,\pm\rangle\propto|\alpha\rangle$
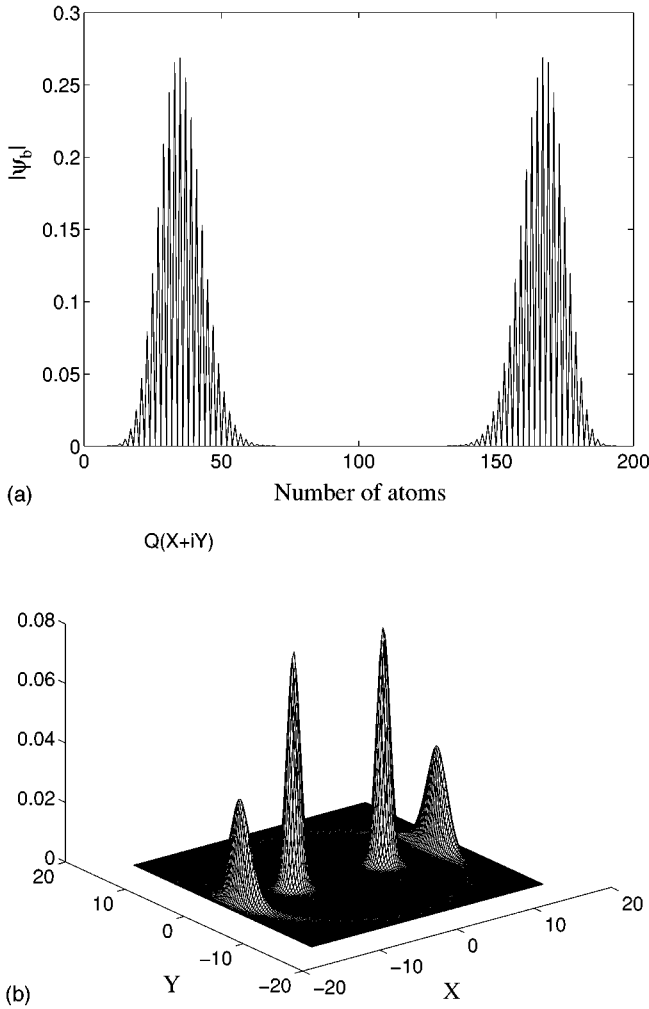
(a)

Q(X+iY)

(b)

FIG. 2. Stochastic simulations of the detections of spontaneously scattered photons for 200 atoms. A typical distribution of (a) the absolute value of the wave function $|\psi_b|$ in the condensate b in the number state basis, and (b) the corresponding Q function after approximately 5000 detections. In (a) two distinct peaks in the number distribution correspond to entangled number state superpositions. The peaks are centered at $N_b \simeq 30$ and at $N_b \simeq 170$ atoms. In the phase-space plotting of the Q function (b) the radius in the xy plane in the polar coordinates is equal to $N_b^{1/2}$ and the polar angle is the relative phase between the two BEC's. The four peaks correspond to the two dominant occupation numbers and two different phase values.

$\pm |-\alpha\rangle$ [27]. These are states which have only even or odd numbers in the atom number distribution and they correspond to superposition states with two different phase values shifted by π.

In Fig. 2(b) we have plotted the corresponding Q function from Eq. (17). The Q function gives the phase-space distribution. The amplitude and phase quadratures are denoted by X and Y. In polar coordinates the radius in the xy plane is equal to $N_b^{1/2}$ and the polar angle is the relative phase between the two BEC's. In Fig. 2(b) it is easy to see the two different sets of peaks corresponding to the two dominating values in the number distribution. All the peaks are aligned parallel to the x axis. This is the reason that two of the four different phase values from Eq. (16) are indistinguishable. Although the distribution in Fig. 2(a) is symmetric, the num-
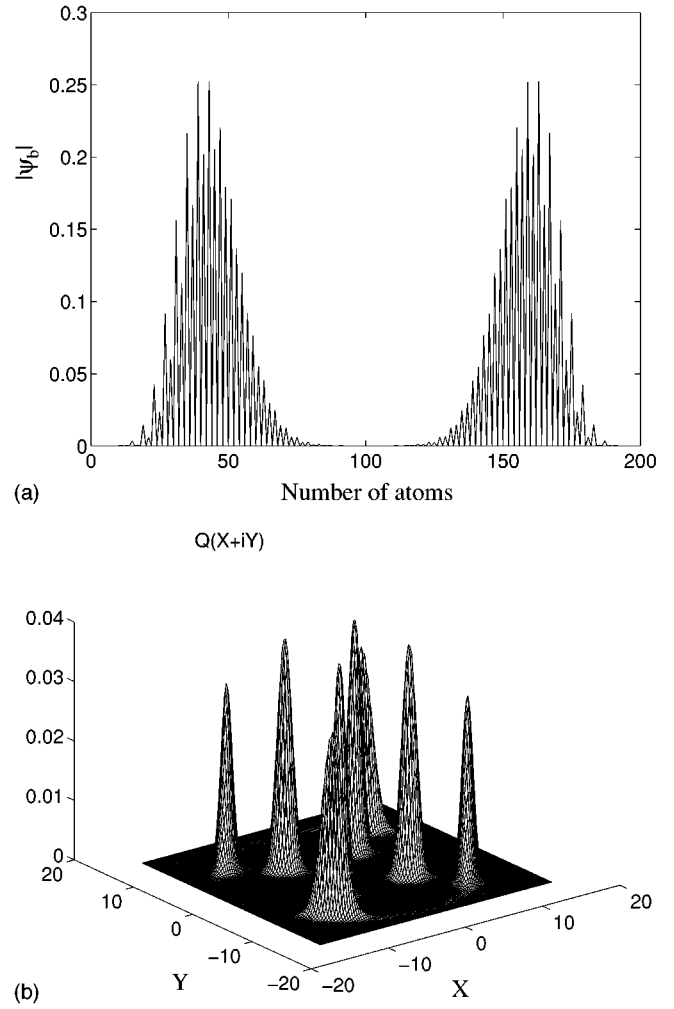
(a)

Q(X+iY)

(b)

FIG. 3. Another representative graph from the same run of measurements with (a) the number state distribution and (b) the Q function. The value of the relative phase has changed from the previous figure. The two entangled number state superpositions and all the four phase values are clearly observed in the Q representation.

ber squeezing of the peak with the larger atom number is much stronger. The fringes indicating a quantum interference in the Wigner distributions [26] are absent in the Q representation, so that graphs of Q functions do not obviously distinguish between pure states and statistical mixtures. However, because we are dealing with basis vectors instead of with density matrices, it is evident that we have a pure state.

In Fig. 3 the distribution in the number state basis and the corresponding Q function are plotted in the same run of measurements as in Fig. 2, but at different times. In Fig. 3(a) two distinct peaks in the number distribution are not as far apart as in Fig. 2(a). In the Q representation, in Fig. 3(b), it is easy to see that the value of the relative phase between the BEC's is different from Fig. 2. In Fig. 3(b) all the four phase values from Eq. (16) are clearly observed. The value of the relative phase between the condensates wanders during the simulations and does not stabilize to any definite value. In Fig. 4 we have one more graph from the same run of measurements. In this case the BEC's are almost in an entangled number state with all the atoms in one of the two condensates. Because the state of the BEC's is closer to a number state than to a
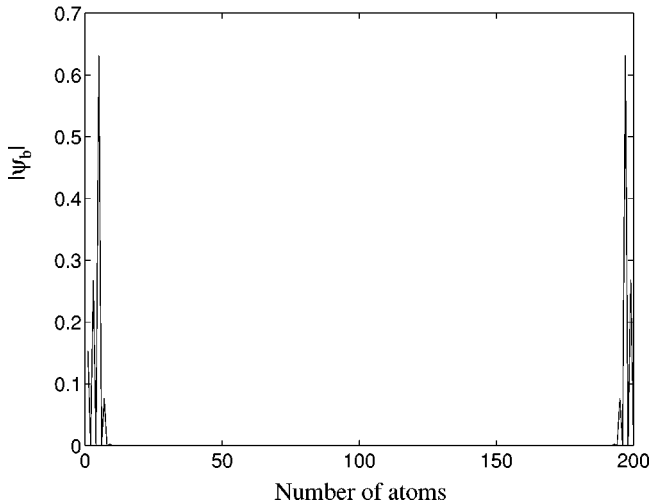
FIG. 4. The same run of measurements as in previous figures. The plotting of an extreme case in which the BEC's are in an entangled number state with almost all the atoms in one of the two condensates.

coherent state, the relative phase is not well defined.

In the calculations we only considered the atom-stimulated scattering to the BEC's. It is not necessarily a well-justified assumption to ignore the unstimulated free-space decay if the condensates contain only 200 atoms. However, the purpose of the numerical simulations was to demonstrate the general properties of the finite systems with a convenient computational efficiency. In the simulations the physical behavior remained qualitatively the same even though the number of atoms was significantly increased. In the real experiments BEC's have typically contained many more than 200 atoms [1–4].

The interaction of the BEC's with their enviroment creates dissipation and the decoherence of the macroscopic superpositions [28]. Decoherence by amplitude damping or by phase damping has been estimated by Walls and Milburn [29]. The amplitude damping corresponds to the losses of atoms from the BEC's. In this case the off-diagonal elements of the density matrix between two coherent states may be shown to be dephased by the factor $\langle\alpha|\beta\rangle^{1-\exp(-\lambda t)}$, where λ is the loss rate for atoms. The phase damping may, e.g., be a consequence of elastic two-body collisions in which a noncondensate atom collides with a condensate atom. In this case the off-diagonal elements of the density matrix between two coherent states with unequal atom numbers N_1 and N_2 are damped by the factor $\exp\{-\lambda(N_1-N_2)^2t/2\}$. These are examples of the decoherence of the ensemble averages over the measurement processes. If decoherence can be associated with measurements, evolution of single realizations may be analyzed by stochastic evolutions of state vectors [30]. Although the decoherence of number state superpositions of the BEC's may exhibit some interesting features, we do not consider this in the present paper.

D. Detection of number state superpositions

In this section we consider the detection of the number state superpositions. The phase superpositions could in principle be measured by simply interfering with the conden-

sates. However, the different phase superpositions correspond to either even or odd coherent states. As explained previously, these are states which have only even or odd numbers in the atom number distribution. Thus, in practice the losses of atoms from the BEC's could shift the fringes and wipe out the qualitative features from the interference pattern.

The existence of the number state superpositions could be verified, for instance, by considering the intensity correlations of the scattered light from the two BEC's. If we assume that the condensates are flying apart and that they are already spatially separated, the amplitude of the spontaneously scattered light field from the condensate b has roughly the dependence $|\mathbf{E}_b^+|\propto\mathcal{E}d_{eg}/(\hbar\Delta)b^\dagger b$, and from the condensate c $|\mathbf{E}_c^+|\propto\mathcal{E}d_{eg}/(\hbar\Delta)c^\dagger c$ [20]. Here we have again considered only the coherent spontaneous scattering of atoms to the BEC's stimulated by large atom numbers; i.e., scattering to the noncondensate c.m. states has been ignored. Because the BEC's are now spatially separated, only the scattering processes in which an atom scatters back to the same condensate are included. We consider a direct counting of photons which is different from, e.g., the phase-contrast imaging [17] used at MIT in a nondestructive optical detection of a BEC. The transmitted probe beam could be blocked by a thin wire as in the dark-ground imaging technique [31]. The scattered light from the two spatially separated BEC's is collected on different photon detectors and the intensity correlations are obtained from the time correlations of the photon counts as in the Hanbury Brown and Twiss experiments [26].

For a number state $|N/2,N/2\rangle$ with large N, the intensities of the scattered light from the spatially separated condensates b and c are approximately $\langle I_b\rangle\sim\langle I_c\rangle\propto(N/2)^2$. The intensity correlations satisfy $\langle I_bI_c\rangle\propto(N/2)^4$. For an entangled number state $(|N-k,k\rangle+|k,N-k\rangle)/\sqrt2$ we have $\langle I_b\rangle\sim\langle I_c\rangle\propto\{(N-k)^2+k^2\}/2\geqslant(N/2)^2$ and $\langle I_bI_c\rangle\propto(N-k)^2k^2\leqslant(N/2)^4$. An especially interesting case is the situation in which the superpositions are far apart: $k\ll N/2$. Then, $\{(N-k)^2+k^2\}/2\simeq2(N/2)^2$ and $(N-k)^2k^2\ll(N/2)^4$. Thus, for the present case of spatially separated condensates the scattering rate from each BEC is larger than the scattering rate given by $N/2$ atoms; on the other hand, the intensity correlations are at the same time strongly reduced. These conclusions are also valid for the case where the superpositions are of coherent states instead of number states, as long as the overlap between the superpositions is negligible.

Because the detection of the number state superpositions relies on atom-stimulated scattering to the BEC's, the entanglement between the condensates is not destroyed in the measurement process. However, the light scattering still creates decoherence by phase damping explained in the preceding section. This decoherence may be reduced by balancing the detection rates of scattered light from the BEC's.

III. CONCLUSIONS

We have shown that two BEC's can be driven into macroscopic superpositions of number and phase states by measurements of spontaneously scattered light. The number state superpositions are entangled and spatially nonlocal ''Schrödinger-cat'' states with high occupation numbers. No stable relative phase between the BEC's is established for a finite system and in the extreme case the condensates approach a number state with almost all the atoms in one of the

BEC's. This is an example of the strong effect of measurements on the state of the condensates. For a finite system detections necessarily perturb the phase and the particular phase measurement process is used is not irrelevant; because different measurement procedures may affect the system in very different ways, the kind of coherence properties, if any, that are established in a detection process are not evident *a priori*.

In the system considered in Ref. [12] two BEC's are in two different Zeeman levels and two phase-coherent laser beams drive Raman transitions between the condensates. In that case the relative phase between the two BEC's is established by measurements of spontaneously scattered photons, even though the condensates have initially well-defined numbers of atoms. In the present paper the large fluctuations of the number difference between the BEC's in the case of a finite system lead to a randomly drifting relative phase. The measurement scheme considered here, with only one laser beam and the two BEC's differing in their external quantum numbers, is closer to the experimental setup used at MIT in a nondestructive optical detection of a BEC [31,17]. In the phase-contrast [17] or dark-ground [31] imaging of the BEC's the role of the mirrors is played by a lens. Although so far all measurements of the interference pattern of BEC's have been destructive, nondestructive measurements could possibly be performed in the near future. Only with nondestructive imaging could one measure how the system evolves in time as a result of the detection process.

[1] M. H. Anderson, J. R. Ensher, M. R. Matthews, C. E. Wieman, and E. A. Cornell, Science **269**, 198 (1995).

[2] K. B. Davis, M.-O. Mewes, M. R. Andrews, N. J. van Druten, D. S. Durfee, D. M. Kurn, and W. Ketterle, Phys. Rev. Lett. **75**, 3969 (1995).

[3] M.-O. Mewes, M. R. Andrews, N. J. van Druten, D. M. Kurn, D. S. Durfee, and W. Ketterle, Phys. Rev. Lett. **77**, 416 (1996).

[4] C. C. Bradley, C. A. Sackett, and R. G. Hulet, Phys. Rev. Lett. **78**, 985 (1997).

[5] J. Javanainen and S. M. Yoo, Phys. Rev. Lett. **76**, 161 (1996); S. M. Yoo, J. Ruostekoski, and J. Javanainen, J. Mod. Opt. (to be published).

[6] M. Naraschewski, H. Wallis, A. Schenzle, J. I. Cirac, and P. Zoller, Phys. Rev. A **54**, 2185 (1996).

[7] J. I. Cirac, C. W. Gardiner, M. Naraschewski, and P. Zoller, Phys. Rev. A **54**, R3714 (1996).

[8] M. W. Jack, M. J. Collett, and D. F. Walls, Phys. Rev. A **54**, R4625 (1996).

[9] T. Wong, M. J. Collett, and D. F. Walls, Phys. Rev. A **54**, R3718 (1996).

[10] Y. Castin and J. Dalibard, Phys. Rev. A **55**, 4330 (1997).

[11] M. J. Steel and D. F. Walls, Phys. Rev. A **56**, 3832 (1997).

[12] J. Ruostekoski and D. F. Walls, Phys. Rev. A **56**, 2996 (1997).

[13] J. Javanainen, Phys. Rev. A **54**, R4629 (1996).

[14] A. Imamoḡlu and T. A. B. Kennedy, Phys. Rev. A **55**, R849 (1997).

[15] J. Ruostekoski and D. F. Walls, Phys. Rev. A **55**, 3625 (1997).

[16] C. M. Savage, J. Ruostekoski, and D. F. Walls, Phys. Rev. A **56**, 2046 (1997).

[17] M. R. Andrews, C. G. Townsend, H.-J. Miesner, D. S. Durfee, D. M. Kurn, and W. Ketterle, Science **275**, 637 (1997).

[18] R. J. Glauber, Phys. Rev. **130**, 2529 (1963); **131**, 2766 (1963); P. L. Kelley and W. H. Kleiner, Phys. Rev. **136**, A316 (1964).

[19] J. I. Cirac, M. Lewenstein, K. Mølmer, and P. Zoller, Phys. Rev. A (to be published).

[20] J. Javanainen and J. Ruostekoski, Phys. Rev. A **52**, 3033 (1995).

[21] J. Ruostekoski and J. Javanainen, Phys. Rev. A **55**, 513 (1997); **56**, 2056 (1997).

[22] J. Dalibard, Y. Castin, and K. Mølmer, Phys. Rev. Lett. **68**, 580 (1992).

[23] C. W. Gardiner, A. S. Parkins, and P. Zoller, Phys. Rev. A **46**, 4363 (1992).

[24] H. J. Carmichael, in *An Open Systems Approach to Quantum Optics*, Lecture Notes in Physics Vol. 18 (Springer, Berlin, 1993).

[25] A. J. Leggett and F. Sols, Found. Phys. **21**, 353 (1991).

[26] D. F. Walls and G. J. Milburn, *Quantum Optics* (Springer, Berlin, 1994).

[27] U. M. Titulaer and R. J. Glauber, Phys. Rev. **145**, 1041 (1966).

[28] W. H. Zurek, Phys. Today **44**(10), 36 (1991), and references therein.

[29] D. F. Walls and G. J. Milburn, Phys. Rev. A **31**, 2403 (1985).

[30] B. M. Garraway and P. L. Knight, Phys. Rev. A **50**, 2548 (1994).

[31] M. R. Andrews, M.-O. Mewes, N. J. van Druten, D. S. Durfee, D. M. Kurn, and W. Ketterle, Science **273**, 84 (1996).